POLYSSACHARIDE-BASED MAGNETIC HYDROGELS AS POTENTICAL VECTORS FOR EXTERNAL-CONTROLLED SOLUTE RELEASE

Alexandre T. Paulino[1,2], Laurence A. Belfiore[2], Matt J. Kipper[2] and Elias B. Tambourgi[1]
[1]*School of Chemical Engineering, Department of Chemical System Engineering, Separation Process Laboratory*
State University of Campinas, Av. Albert Einstein, 500, Bloco A, Cidade Universitária, Campinas, SP 13083-852, Brazil
[2]*Department of Chemical & Biological Engineering, Polymer Physics & Engineering Laboratory*
Colorado State University, Fort Collins, CO 80523, U.S.A.

Keywords: Magnetic hydrogel, Polysaccharide, External-controlled solute release.

Abstract: This work describes the synthesis of polysaccharide-based magnetic hydrogels with the introduction of magnetite nanoparticles in the polymer network. The magnetic hydrogels were characterized by Fourier-transform infrared spectroscopy (FTIR) and magnetization curves. FTIR analysis confirmed the efficiency of the polysaccharide-modifying process. The amounts of diffused water into or out-of a hydrogel network were measured. The degree of swelling of the polysaccharide-based magnetic hydrogels was less than that found for the regular polysaccharide-based hydrogels and there was no variation in the water diffusion mechanism. The absence of hysteresis loops and coercivity observed through magnetization curves indicated that magnetic hydrogels can be applied in external-controlled solute release.

1 INTRODUCTION

In recent years, there has been substantial interest in the potential applications of functionalized hydrogels. These types of hydrogels have many important properties and offer advantages over non-functionalized hydrogels (Chaterji et al., 2007); (Bajpai et al., 2008). The advantages of such hydrogels have been observed through some studies on controlled drug release systems, cell proliferation, water treatment, soil conditioning and so forth. (Oh et al., 2008); (Arizaga et al., 2010); (Deligkaris et al., 2010).

Functionalized hydrogels based on polysaccharides, proteins and amino acids have been extensively studied for medical, pharmaceutical and biological application due to their properties of biocompatibility with living organisms, biodegradability, accessibility and renewability (Morelli and Chiellini, 2010). In this contribution, external magnetic field-sensitive functionalized hydrogels based on gum arabic, chitosan and maltodextrin were synthesized with the introduction of magnetite nanoparticles in the polymer network. The potentiality of these hydrogels as magnetic vectors for external-controlled solute release was investigated by FTIR, magnetization curves and water absorption kinetic.

2 EXPERIMENTAL PROCEDURES

2.1 Materials

Chitosan (Aldrich), acetic acid (Merck), acrylic acid (Merck), glycidyl methacrylate (Across Organics), methylenebisacrylamide (Merck), hydrochloric acid (Merck), ammonium persulfate (Aldrich), gum arabic (Sudan), sodium hydroxide (Nuclear), acrylamide (Aldrich), potassium acrylate (Aldrich), maltodextrin (Aldrich), ethanol (TEDIA), magnetite nanoparticles (Fe_3O_4) purchased from Fisher Scientific and characterized elsewhere (Paulino et al., 2009). All experiments were performed using Milli-Q® water.

2.2 Hydrogel Synthesis

1% chitosan solution was prepared by diluting the

T. Paulino A., A. Belfiore L., J. Kipper M. and B. Tambourgi E..
POLYSSACHARIDE-BASED MAGNETIC HYDROGELS AS POTENTICAL VECTORS FOR EXTERNAL-CONTROLLED SOLUTE RELEASE.
DOI: 10.5220/0003870802630268
In *Proceedings of the International Conference on Biomedical Electronics and Devices* (BIODEVICES-2012), pages 263-268
ISBN: 978-989-8425-91-1

appropriate amounts of the polysaccharide with acetic acid in a 50-mL beaker. Gaseous nitrogen was purged into the system for 30 min in order to remove the dissolved oxygen. Known amounts of ammonium persulfate were then introduced to initiate chitosan for the generation of radicals. The complete polymerization reaction took place at 70 ºC for three hours after adding 15 mL of Milli-Q® water, acrylic acid, methylene-bis-acrylamide and magnetite nanoparticles. The hydrogel was purified and dried in an oven at 50 ºC for 12 to 24 hours.

Prior to synthesizing the hydrogels based on either gum arabic or maltodextrin, the specific polysaccharide was modified through functionalization using glycidyl methacrylate (Dorkoosh et al., 2002_a, 2002_b). Each synthesis was carried out through the solubilization of the specific modified polysaccharide in an aqueous solution containing acrylamide, potassium acrylate, ammonium persulfate and magnetite nanoparticles. The solution was heated to 65 °C for some minutes under constant stirring. The hydrogel obtained was purified and dried in an oven at 50 ºC for 12 to 24 hours.

2.3 Water Uptake Mechanism

Pieces of previously dried hydrogel with masses ranging from 50 to 100 mg were placed in contact with 100 mL of water for different contact times, with pH controlled at around 6.5. The degree of swelling (DS) was calculated using Eq. 1:

$$DS = \frac{m_s - m_d}{m_d} \quad (1)$$

in which m_s and m_d are the masses of swollen and dried hydrogel, respectively.

The absorption mechanism of water in a three-dimensional hydrogel structure has been described based on the diffusion phenomena and macromolecular relaxation of the three-dimensional structure. This approach is related to Fickian diffusion processes, in which the coefficient (*n*) is a parameter that describes the adsorption mechanism (Hallinan et al., 2010), the values (1/min) of which are determined from the fraction curves of diffused water (M_t/M_{eq}) in function of time, as presented mathematically in Eq. 2:

$$\frac{M_t}{M_{eq}} = kt^n \quad (2)$$

in which M_t and M_{eq} are the masses (g) of water absorbed by a hydrogel at a specific time and in equilibrium, respectively, and k (dimensionless) is the proportionality constant of the polymer network of a particular hydrogel.

The Fickian diffusion model sets the absorption of water in a three-dimensional structure until 70 % of initial absorption. Above 70 %, there is no linearity in the graph curve $\ln(M_t/M_{eq})$ versus time (t). The linear regression of Eq. 2 is seen in Eq. 3:

$$\log\left(\frac{M_t}{M_{eq}}\right) = \log K + n \log(t) \quad (3)$$

The *n* values for different released solutes have been commonly characterized by Fickian diffusion, non-Fickian diffusion (anomalous) and Super Case II models. For *n* values equal to 0.45, the solute transport is characterized by the Fickian diffusion model. In this case, it is considered that water molecules may simply diffuse through the polymer network by diffusion processes. For *n* values between 0.45 and 0.89, the solute diffusion is characterized by the non-Fickian diffusion model. In this case, the diffusion mechanism is characterized by two processes occurring simultaneously – diffusion through the pores and macromolecular structure relaxation. When the phenomenon of macromolecular relaxation is involved, there is a direct relationship with the flexibility of the polymer network. Finally, when the *n* value is higher than 0.89, the diffusion mechanism of solutes in three-dimensional polymer structures is governed exclusively by macromolecular structure relaxation, i.e., Super Case II model (Halligan et al., 2010; Paulino et al., 2011).

2.4 FTIR Analysis

The samples of the polysaccharide-based hydrogels were characterized in potassium bromide pellets using FTIR spectra (FT-GO_{max} Bomem Easy MB−100, Nickelson). To achieve the best resolution (4.0 cm^{-1}), 21 scans min^{-1} were run for each spectrum.

2.5 Magnetization Analysis

Magnetization curves for the polysaccharide-based magnetic hydrogel were measured using a vibrating-sample magnetometer (physical properties measurement system (PPMS)−9, Quantum Design, SQID magnetometer), with a maximal magnetic field of 7 T and sensibility of 10^{-6} emu at a temperature of 573 K.

3 RESULTS AND DISCUSSIONS

3.1 Degree of Swelling

The degree of swelling decreased from 8.78 to 6.48 g of water per gram of chitosan-based dried hydrogel concurrently with the increase in magnetite concentration from 0.0 to 5.5 wt.-%, respectively. The degree of swelling of the chitosan-based magnetic hydrogels was less than that found for the chitosan-based hydrogel without magnetic behavior (0 wt.-% of magnetite). The same behavior was observed with hydrogels based on modified maltodextrin and modified gum arabic, as a lesser degree of swelling occurred in magnetic hydrogels.

An electrostatic repulsion generated between the ionized groups of both the magnetic hydrogels and the hydrogels without magnetic properties may expand the polymer network (Jiang et al., 2010). This phenomenon helps destabilize the structures of the material, thereby allowing the diffusion of water and solutes in and out-of the polymer matrix (Paulino et al., 2009; 2010). Thus, a greater amount of magnetite used in the hydrogel synthesis leads to a greater degree of crosslinking due to the formation of covalent bonds between the iron and hydroxyl or amine groups. With this logic, a greater density of crosslinking decreases the swelling rate.

3.2 Water Diffusion Mechanism

Table 1: Water diffusion exponent values (n) at 25 ^{o}C into hydrogels based on chitosan, modified maltodextrin and modified gum arabic (pure hydrogel) and with known amounts of magnetite (magnetic hydrogel).

Chitosan-based hydrogel (Pure hydrogel) and magnetic hydrogels		
	(n)	(R^2)
Pure hydrogel	0.5478	0.9918
1.9 wt.-% magnetite	0.5474	0.9907
2.9 wt.-% magnetite	0.5910	0.9841
5.5 wt.-% magnetite	0.6046	0.9885
Modified-maltodextrin-based hydrogel (Pure hydrogel) and magnetic hydrogels		
	(n)	(R^2)
Pure hydrogel	0.5430	0.9950
1.9 wt.-% magnetite	0.5545	0.9993
2.9 wt.-% magnetite	0.5479	0.9973
5.5 wt.-% magnetite	0.5492	0.9982
Modified-gum-arabic-based hydrogel (Pure hydrogel) and magnetic hydrogels		
	(n)	(R^2)
Pure hydrogel	0.6201	0.9982
1.9 wt.-% magnetite	0.6307	0.9927
2.9 wt.-% magnetite	0.6385	0.9857
5.5 wt.-% magnetite	0.6496	0.9921

Table 1 displays the water diffusion exponent (n) for hydrogels based on chitosan, modified maltodextrin and modified gum arabic, containing magnetite concentrations ranging from 0.0 to 5.5 wt.-%. The n values ranged from 0.5430 to 0.6496, indicating the non-Fickian diffusion model, with a tendency toward macromolecular structure relaxation. Moreover, these results indicate that there is no variation in the water diffusion mechanism between regular and magnetic hydrogels, confirming previous studies (Paulino et al., 2009; 2010; 2011).

3.3 FTIR Analysis

Fig. 1 displays the FTIR spectra of the chitosan-based hydrogel and chitosan-based magnetic hydrogel. All hydrogels exhibited a broad absorption band between 1715 and 1724 cm^{-1}, corresponding to the carbonyl group stretch in protonated carbonyl acid, which means that these hydrogels are polycations. This carbonyl comes from the acetylated chitosan with a 10% degree of acetylation. In the chitosan-based magnetic hydrogel spectrum, the peak shifted to lower values due to hydrogen bonds and interactions with magnetite nanoparticles. The band appearing at 1574 cm^{-1} corresponds to the amine group vibrations (amide II) in the chitosan molecule, which interacted with magnetite nanoparticles, appearing at 1552 cm^{-1} in the magnetic hydrogel spectrum. The band at 1451 cm^{-1} may be attributed to the methyl groups. The peak at 1401 cm^{-1} may be associated to CH_2 scissoring of the six carbons of the glucosamine residues. The sharp bands around 1322 cm^{-1} reveal the presence of carboxylic groups and appeared at 1249 cm^{-1} in the magnetic hydrogel spectrum due the interaction with the magnetite nanoparticles. The remaining broad absorption bands between 1110 and 1155 cm^{-1} may be associated to vibration modes of the saccharide rings and C-N stretching. The C-O-C stretching vibration is also expected to take place around 1000 cm^{-1} and appears as a small shoulder on the broad absorption band. There were important differences between the chitosan-based hydrogel and chitosan-based magnetic hydrogel spectra, which were used to characterize the modification achieved with the embedding of magnetite nanoparticles. The main differences were related to the shifting to lower values of the absorption bands at 1724, 1574 and 1322 cm^{-1} due the formation of covalent bonds with magnetite molecules.

Fig. 2 displays the FTIR spectra of the purified maltodextrin, glycidyl methacrylate, modified maltodextrin and modified maltodextrin-based

magnetic hydrogels. The band appearing at 1649 cm^{-1} in the purified maltodextrin spectrum corresponds to the C-OH group stretching of polysaccharides. The absorption band at 1452 cm^{-1} was attributed to the methyl groups and the band at 1420 cm^{-1} was attributed to CH_2 scissoring. The peak at 1371 cm^{-1} may be attributed to -OH in plane bending vibration. These peaks were also noted in the modified maltodextrin spectrum. Moreover, purified maltodextrin, modified maltodextrin and modified maltodextrin-based magnetic hydrogels exhibited similar peaks between 1025 and 1245 cm^{-1}. The C-O group stretching may appear at ~1245 cm^{-1}.

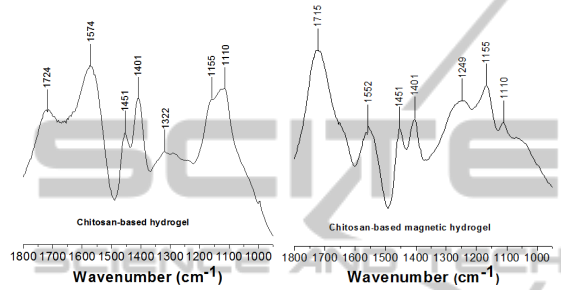

Figure 1: Transmission FTIR spectra for chitosan-based hydrogel and chitosan-based magnetic hydrogel.

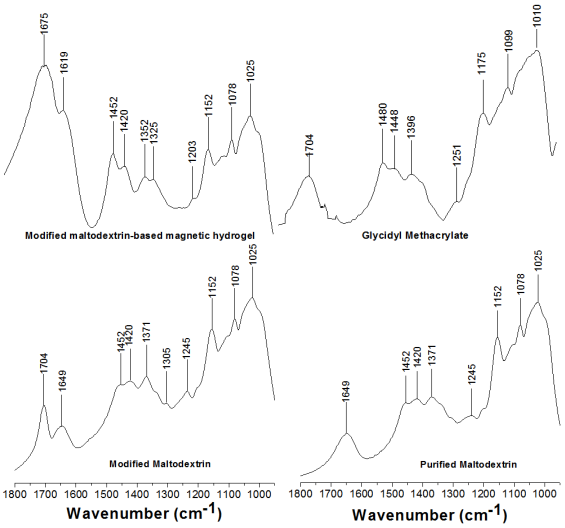

Figure 2: Transmission FTIR spectra for modification of purified maltodextrin with glycidyl methacrylate and modified maltodextrin-based magnetic hydrogels.

Absorption bands between 1000 and 1152 cm^{-1} may be attributed to ether bonds. These bands were also observed in the modified maltodextrin-based magnetic hydrogel. After the modification of purified maltodextrin using glycidyl methacrylate, a new absorption band appeared at 1704 cm^{-1}, which was attributed to carbonyl stretching of the conjugated ester groups derived from a glycidyl methacrylate molecule. The appearance of this band was associated to the efficiency of the polysaccharide-modifying process (Chatterjee et al., 2003). The absorption bands at 1704 and 1649 cm^{-1} shifted to lower values (1675 and 1619 cm^{-1}, respectively) after the modified maltodextrin-based magnetic hydrogel synthesis. This was associated to interactions between these specific groups and the magnetite molecules, as previously described in the FTIR spectra for chitosan-based magnetic hydrogels.

Fig. 3 displays the FTIR spectra of the purified gum arabic, glycidyl methacrylate, modified gum arabic and modified gum arabic-based magnetic hydrogels.

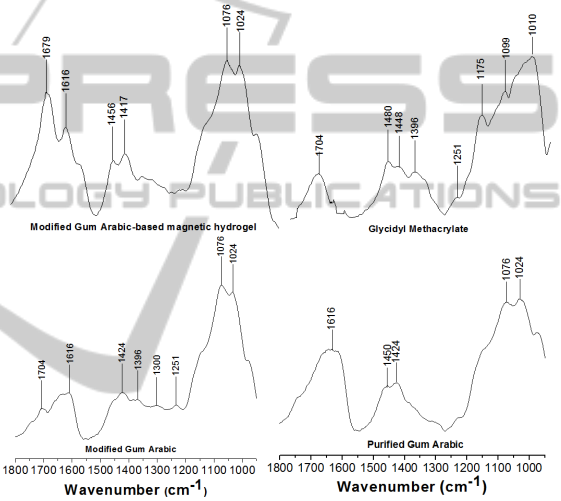

Figure 3: Transmission FTIR spectra for the modification of gum arabic with glycidyl methacrylate and modified gum arabic-based magnetic hydrogels.

Considering the purified gum arabic spectrum, an absorption band at 1616 cm^{-1} was observed, corresponding to the C-OH groups from purified polysaccharides. The absorption bands at 1450 and 1424 cm^{-1} correspond to the methyl groups and CH_2 scissoring, respectively. The bands at 1024 and 1076 cm^{-1} correspond to the ether bond vibrations. The new absorption band at 1704 cm^{-1} appearing in the modified gum arabic spectrum was attributed to the carbonyl stretching frequency of the conjugated ester groups derived from a glycidyl methacrylate molecule. As observed for the modified maltodextrin-based magnetic hydrogel, the absorption bands at 1704 and 1616 cm^{-1} shifted to lower values (1679 and 1616 cm^{-1}, respectively) due the presence of hydrogen bonds and covalent bonds between hydrogel groups and magnetite molecules.

3.4 Magnetization Curves

Fig. 4 displays the magnetization loops [magnetization versus applied magnetic field (B−H)] of the chitosan-, modified maltodextrin- and modified gum arabic-based magnetic hydrogels, containing 1.9 wt.-% magnetite nanoparticles.

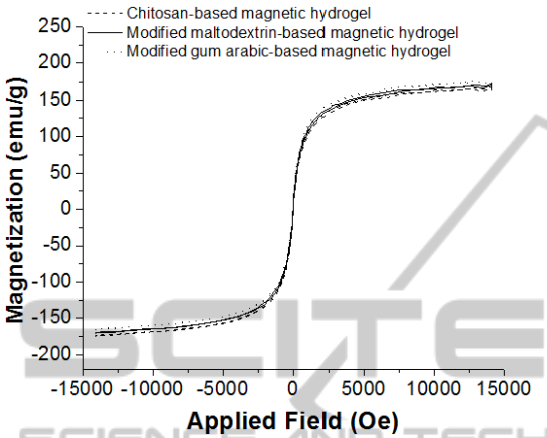

Figure 4: Magnetization *vs.* applied magnetic field for magnetic hydrogels based on chitosan, modified maltodextrin and modified gum arabic; magnetic hydrogels containing 1.9 wt.-% magnetite.

The saturation magnetization values ranged from 150 to 160 emu g^{-1}. Neither remanence nor coercivity was observed for the magnetic hydrogels due to the absence of hysteresis loops. This is a characteristic of nanoparticulate materials embedded in hydrogels (Chatterjee et al., 2003); (Mahkam, 2010). Therefore, it may be assumed that the polysaccharide-based magnetic hydrogels support nanoparticulate structures. It may also be stated that the magnetite nanoparticles embedded in the magnetic hydrogels through covalent bonding are magnetic/superparamagnetic (Chatterjee et al., 2003); (Mahkam, 2010). The superparamagnetic properties supported by the magnetic hydrogels may be directly related to the smaller size of magnetite nanoparticles and their satisfactory dispersion throughout the hydrogel network (Paulino et al., 2010). Otherwise, a lack of either magnetization or superparamagnetic properties would be observed. A ferromagnetic material with either low or no coercivity is said to be soft and may be used in some kind of electronic devices. In many applications, small hysteresis loops are driven around points in the B-H plane. Loops near the origin have greater magnetic permeability (Chatterjee et al., 2003); (Mahkam, 2010).

4 CONCLUSIONS

A hydrogel with and without magnetic properties may be synthesized by conventional methods and characterized through methods such as FTIR, magnetometry and water absorption kinetic studies. Detained FTIR results were particularly useful in demonstrating that the magnetic hydrogels were formed by a cross-linking reaction of the natural polymers in the presence of magnetite nanoparticles. The superparamagnetic properties obtained through magnetization may be directly related to the smaller size of magnetite nanoparticles and their satisfactory dispersion throughout the hydrogel network; otherwise, a lack of either magnetization or superparamagnetic properties would have been observed. A ferromagnetic material with either low or no coercivity is said to be soft and may be used in many kinds of electronic devices. The water uptake analysis revealed that a greater amount of magnetite in the magnetic hydrogel network led to lesser water uptake. On the other hand, a greater amount of magnetite made the hydrogel more sensitive to a externally applied magnetic field. If the main goal of these materials is the application in remote-controlled drug release, it could be supposed that after applying an external magnetic field to a loaded magnetic hydrogel with a specific drug encapsulated in its structure, magnetic spins of magnetite would be aligned in the same direction as the applied magnetic field and, consequently, an enhanced attractive force between north and south poles would narrow the hydrogel network and deliver both water and drug toward-out from the polymer network. Accordingly, remote-controlled drug release can be monitored and controlled by an external applied magnetic field through a non-invasive procedure. Furthermore, the magnetic hydrogels synthesized here could effectively be applied as a magnetic biosorbent, a magnetic biosensor, a soil conditioner or even in cancer cell treatment.

ACKNOWLEDGEMENTS

A. T. Paulino and E. B. Tambourgi thank the State of São Paulo Research Foundation (FAPESP, Brazil) for the post-doctorate fellowship (Process N^0 2008/00285-7). A. T. Paulino, L. A. Belfiore and M. J. Kipper thank the Coordination of Improvement of Higher Education Personnel (CAPES, Brazil) for the post-doctorate fellowship abroad (Process N^0 5267/09-9).

REFERENCES

Arizaga, A., Ibarz, G., Piñol, R., 2010. J. Colloid Interf. *Sci., 348*, 668–672.

Bajpai, A. K., Shukla, S. K., Bhanu, S., Kankane, S., 2008. Prog. Polym. *Sci., 33*, 1088–1118.

Chaterji, S., Kwon, I. K., Park, K., 2007. Prog. Polym. *Sci., 32*, 1083–1122.

Chatterjee, J., Haik, Y., Jen Chen, C., 2003. Colloid Polym. *Sci., 281*, 892–896.

Deligkaris, K., Tadele, T. S., Olthuis, W., van den Berg, A., 2010. *Sensors Act. B*, 147, 765–774.

Dorkoosh, F. A., Coos Verhoef, J., Ambagts, M. H. C., Rafiee-Tehrani, M., Borchard, G., Junginger, H. E., 2002_b. *Eur. J. Pharmaceut. Sci*., 15, 433–439.

Dorkoosh, F.A., Verhoefm, J.C., Borchard, G., Rafiee-Tehrani, M., Verheijden, J.H.M., Junginger, H.E., 2002_a. *Int. J. Pharm*., 247, 47-55.

Hallinan, D. T., De Angelis, M. G., Baschetti, M. G., Sarti, G. C., Elabd, Y. A., 2010. *Macromolecules*, 43, 4667–4678.

Jiang, G. Q., Liu, C., Liu, X. L., Zhang, G. H., Yang, M., Chen, Q. R., Liu, F. Q., 2010. J. Macromol. *Sci. Pure. Appl. Chem.*, 47, 663-670.

Mahkam, M., 2010. J. Bioact. *Compat. Polym.,* 25, 406-418.

Morelli, A., Chiellini, F., 2010. Macromol. *Chem. Phys.,* 211, 821-832.

Oh, J. K., Drumright, R., Siegwart, D. J., Matyjaszewski, K., 2008. *Prog. Polym. Sci*., 33, 448–477.

Paulino, A. T., Fajardo, A. R., Junior, A. P., Muniz, E. C., Tambourgi, E. B., 2011. *Polym. Int*., 60, 1324–1333.

Paulino, A. T., Guilherme, M. R., Almeida, E. A. M. S., Pereira, A. G. B., Muniz, E. C., Tambourgi, E. B., 2009. *J. Magn. Magn. Mater*., 321, 2636 – 2642.

Paulino, A. T., Guilherme, M. R., Mattoso, L. H. C., Tambourgi, E. B., 2010. *Macromol. Chem. Phys.,* 211, 1196-1205.